Follow us @BoneJointRes

Freely available online OPEN ACCESS

BJR

ARTHRITIS

The role of accelerated growth plate fusion in the absence of SOCS2 on osteoarthritis vulnerability

H. J. Samvelyan,
C. Huesa,
L. Cui,
C. Farquharson,
K. A. Staines

From University of Brighton, Brighton, UK

Aims

Osteoarthritis (OA) is the most prevalent systemic musculoskeletal disorder, characterized by articular cartilage degeneration and subchondral bone (SCB) sclerosis. Here, we sought to examine the contribution of accelerated growth to OA development using a murine model of excessive longitudinal growth. Suppressor of cytokine signalling 2 (SOCS2) is a negative regulator of growth hormone (GH) signalling, thus mice deficient in SOCS2 (*Socs2*$^{-/-}$) display accelerated bone growth.

Methods

We examined vulnerability of *Socs2*$^{-/-}$ mice to OA following surgical induction of disease (destabilization of the medial meniscus (DMM)), and with ageing, by histology and micro-CT.

Results

We observed a significant increase in mean number (wild-type (WT) DMM: 532 (SD 56); WT sham: 495 (SD 45); knockout (KO) DMM: 169 (SD 49); KO sham: 187 (SD 56); $p < 0.001$) and density (WT DMM: 2.2 (SD 0.9); WT sham: 1.2 (SD 0.5); KO DMM: 13.0 (SD 0.5); KO sham: 14.4 (SD 0.7)) of growth plate bridges in *Socs2*$^{-/-}$ in comparison with WT. Histological examination of WT and *Socs2*$^{-/-}$ knees revealed articular cartilage damage with DMM in comparison to sham. Articular cartilage lesion severity scores (mean and maximum) were similar in WT and *Socs2*$^{-/-}$ mice with either DMM, or with ageing. Micro-CT analysis revealed significant decreases in SCB thickness, epiphyseal trabecular number, and thickness in the medial compartment of *Socs2*$^{-/-}$, in comparison with WT ($p < 0.001$). DMM had no effect on the SCB thickness in comparison with sham in either genotype.

Conclusion

Together, these data suggest that enhanced GH signalling through SOCS2 deletion accelerates growth plate fusion, however this has no effect on OA vulnerability in this model.

Cite this article: *Bone Joint Res* 2022;11(3):162–170.

Keywords: Osteoarthritis, SOCS2, Cartilage, Growth plate, Bone, Growth hormone

Article focus

- The reversion of chondrocyte behaviour to an earlier developmental-like phenotype in osteoarthritis (OA) has been defined, however the precise contribution of accelerated growth to OA development remains unclear.
- Here, we used a murine model of excessive longitudinal growth (suppressor of cytokine signalling 2 (SOCS2) deletion – a suppressor of growth hormone signalling) and examined their vulnerability to surgical and ageing-related OA development.

Key messages

- We observed a significant increase in number and density of growth plate bridges in *Socs2* knockout mice in comparison to wild-type (WT), thus indicating accelerated growth plate fusion in this model.
- Histological examination of *Socs2* knockout and WT knee joints revealed similar articular cartilage lesion severity and osteophyte formation scores, and therefore no effect of accelerated growth in this model on articular cartilage damage.

Correspondence should be sent to Katherine Ann Staines; email: k.staines@brighton.ac.uk

doi: 10.1302/2046-3758.113.BJR-2021-0259.R1

Bone Joint Res 2022;11(3):162–170.

Strengths and limitations

- This study reported, for the first time, accelerated growth plate fusion in *Socs2* knockout mice in which an excessive growth phenotype is observed.
- A limitation of this study is the complexity of the GH/insulin-like growth factor 1 (IGF-1) signalling pathway in OA, thus highlighting the need for a better understanding of its role in disease pathology.

Introduction

Osteoarthritis (OA) is the most prevalent systemic musculoskeletal disorder, characterized by degeneration of joint articular cartilage, osteophyte formation, subchondral bone plate thickening, synovial proliferation, and inflammation. OA has a multifactorial aetiology including ageing, trauma, obesity, and heredity. Further, a complex interplay of major molecules and signalling pathways play indispensable roles in OA development.[1-5] Despite this, effective disease-modifying treatments are currently limited.

Endochondral ossification is an essential process for longitudinal bone growth. It requires hypertrophic differentiation of chondrocytes, characterized by secretion of type X collagen (COL10A1), matrix metalloproteinase-13 (MMP-13), and vascular endothelial growth factor (VEGF), followed by the subsequent degradation and conversion of the growth plate cartilage matrix into highly vascularized bone tissue.[6,7] With sexual maturation, the human growth plate undergoes progressive narrowing as bony bridges form and span its width, establishing continuity between the cancellous bone of the epiphysis and metaphysis.[8] These growth plate bridging events ultimately lead to complete growth plate closure and cessation of human growth.[9] OA is widely accepted to involve the reversion of chondrocyte behaviour to an earlier developmental-like phenotype, which could drive the disease process. Indeed, re-expression of the type IIA procollagen, a spliced variant of the type II collagen gene (COL2A1) normally expressed in chondroprogenitor cells, in adult osteoarthritic articular chondrocytes indicates reversion of these cells to early developmental-like phenotype.[10]

Consistent with this, Staines et al[11] have previously shown the abnormal deployment of a transient chondrocyte phenotype in the joints of a STR/ort mouse, a murine model for spontaneous OA.[12] Staines et al[11] further revealed accelerated long bone growth, a wider zone of growth plate proliferative chondrocytes, and widespread COL10A1 and MMP-13 expression beyond the expected hypertrophic zone distribution in these mice, which may underpin their OA onset. However, the precise contribution of accelerated growth to OA development remains unclear.

Suppressor of cytokine signalling 2 (SOCS2), one of the members of the suppressor of cytokine signalling family glycoproteins, is implicated in cancer and disorders of immune system and central nervous system.[13-15] SOCS2 has been shown as a primary intracellular suppressor of the growth hormone (GH) signalling pathway, thus mice deficient in SOCS2 (*Socs2*$^{-/-}$) display an excessive growth phenotype.[16] Here, we use this mouse model of accelerated bone growth to understand the association between aberrant growth dynamics and OA development. To achieve this, we examined the vulnerability of *Socs2*$^{-/-}$ mice to OA following surgical induction of disease (destabilization of the medial meniscus (DMM)), and with ageing, by histology and micro CT.

Methods

Animals. *Socs2-/-* mice on a C57/BL6 genetic background were generated as previously described.[17] For genotyping, tail-biopsied DNA was analyzed by polymerase chain reaction (PCR) for *Socs2* wild-type (WT) (Forward: TGTTTGACTGAGCTCGCGC, Reverse: CAACTTTAGTGT CTTGGATCT) or the neocassette (*Socs2 –/–*; Forward: ACCCTGCACACTCTCGTTTTG, Reverse: CCTCGACTAAAC ACATGTAAAGC). Mice were kept in polypropylene cages, with light/dark 12-hour cycles, at 21°C (± 2°C), and fed ad libitum with maintenance diet (Special Diet Services, UK). Ageing studies were completed in 12- to 13-month-old *Socs2-/-* (n = 6) and C57/BL6 WT (n = 6) male mice (Charles River, UK). Analyses were conducted blindly to minimize the effects of subjective bias. All experimental protocols were approved by the local ethics committee, and the animals were maintained in accordance with UK Home Office guidelines for the care and use of laboratory animals. Animal studies were conducted in line with the ARRIVE guidelines.

Destabilization of the medial meniscus. Eight-week-old *Socs2-/-* and C57/BL6 WT male mice (Charles River) were randomally allocated into 1) surgically induced DMM under isoflurane-induced anaesthesia (n = 6/genotype) or 2) sham operated (n = 6/genotype) groups. Following transection of the medial meniscotibial ligament to destabilize the medial meniscus, the left knee joint capsule and skin were closed and anaesthesia reversed. Sham-operated joints were used as controls. After eight weeks, knee joints were dissected, fixed in 4% paraformaldehyde for 24 hours at 4°C, and then stored in 70% ethanol.

Micro-CT analysis. Scans of the right knee joint were performed with an 1172 X-Ray microtomograph (SkyScan, Belgium) to evaluate the subchondral bone. High-resolution scans with voxel size of 5 µm were acquired (50 kV, 200µA, 0.5 mm aluminium filter, 0.6° rotation angle). The projection images were reconstructed using NRecon software version 1.6.9.4 (SkyScan). Each dataset was rotated in DataViewer (SkyScan) to ensure similar orientation and alignment for analysis. Regions of interest (ROIs) were hand-drawn of the subchondral trabecular bone in the medial and lateral compartments of the femur and tibia. Subchondral bone ROIs were subsequently selected for each compartment. Analysis of subchondral bone plate thickness and the epiphyseal trabecular bone was achieved using 3D algorithms in CTAn

Table I. Weights of wild type and Socs2$^{-/-}$ (knockout) mice during eight-week post-destabilization of the medial meniscus experimental timeline.

Variable	Mean weight, g (SD)								
Week	**0**	**1**	**2**	**3**	**4**	**5**	**6**	**7**	**8**
WT sham	23.2 (0.4)	22.2 (1.0)	24.0 (0.4)	25.6 (0.5)	26.4 (0.7)	27.0 (0.7)	27.6 (0.8)	28.2 (0.8)	29.0 (0.7)
WT DMM	22.4 (0.3)	21.8 (0.3)	23.0 (0.3)	24.0 (0.4)	24.5 (0.3)	24.9 (0.3)	25.6 (0.4)	25.7 (0.3)	26.5 (0.3)
KO sham	32.3 (1.2)	33.6 (0.9)	34.8 (1.1)	35.0 (1.0)	36.4 (1.1)	38.1 (1.3)	38.7 (0.9)	39.0 (0.9)	40.4 (0.9)
KO DMM	31.3 (0.8)	33.0 (0.7)	33.7 (0.7)	34.9 (1.0)	35.8 (1.0)	39.8 (0.6)	38.3 (1.1)	38.9 (1.1)	40.3 (1.0)

DMM, destabilization of the medial meniscus; KO, knockout; SD, standard deviation; WT, wild type.

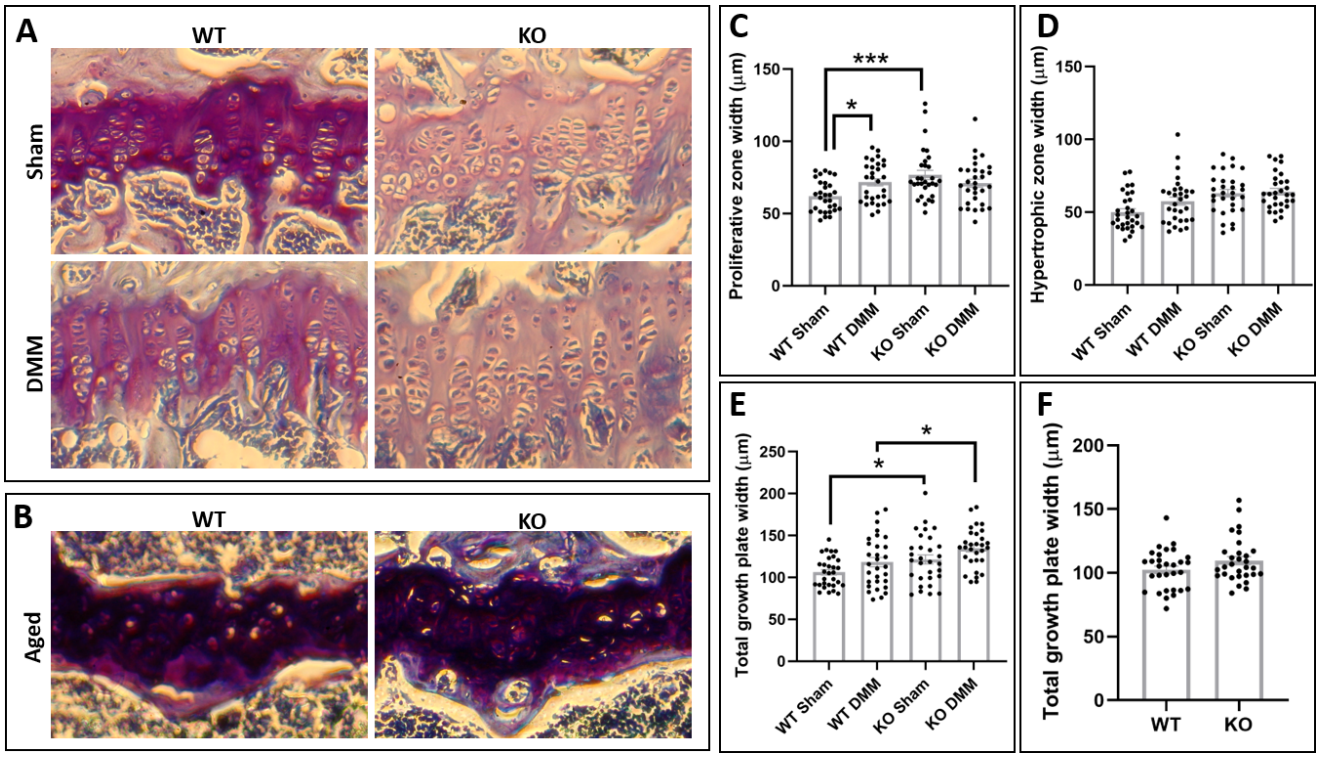

Fig. 1

Socs2-deficient mice exhibit widened growth plates. Histological images of toluidine blue stained growth plates in a) wild type (WT) and Socs2$^{-/-}$ (knockout (KO)) destabilization of medial meniscus (DMM) and sham mice, and b) aged WT and KO mice (10×). Reduced staining in the KO growth plates suggests reduced proteoglycans in these animals. Quantification of c) proliferative zone, d) hypertrophic zone, and e) total growth plate width in WT and KO DMM and sham mice. f) Quantification of total growth plate width in aged WT and KO mice. Data are presented as mean and standard error of the mean. One-way analysis of variance was used for DMM/sham animals and an independent-samples *t*-test for aged animals. *p < 0.05 ***p < 0.001.

(SkyScan) to provide: subchondral bone plate thickness (SCB Th., mm); subchondral bone plate bone volume/tissue volume (SCB BV/TV, %); epiphyseal trabecular bone volume/tissue volume (Tb. BV/TV, %); trabecular number (Tb. N., mm^{-1}); trabecular thickness (Tb. Th., mm); and trabecular separation (Tb. Sp., mm).

Growth plate bridging analysis. Growth plate bridging analysis was conducted using a 3D micro-CT quantification method as previously described.[8,18] Briefly, micro-CT scans of the tibiae were segmented using a region-growing algorithm within the Avizo (V8.0, Thermo Fisher Scientific, USA) software. The central points of all bony bridges were identified (Supplementary Figure a) and projected on the tibial joint surface. The distribution of the areal number density of bridges (N, the number of bridges per 256 µm × 256 µm window) was then calculated and superimposed on the tibial joint surface (each bridge has a colour that represents the areal number density at the bridge location).

Histological analysis. Murine left knee joints were decalcified in 10% ethylenediaminetetraacetic acid (EDTA) for approximately four weeks at 4°C, wax-embedded and 6 µm coronal sections cut. For assessment of OA severity, multiple sections (> 5/slide) from 120 µm intervals across the whole joint were stained with Toluidine blue (0.4% in 0.1 M acetate buffer, pH 4). The total width of the growth plate, as well as the proliferating and hypertrophic zones, were measured at ten different points along the length of the growth plate based on established cell morphology.[19] This was conducted in 6 µm coronal sections from the middle region of the knee joint in a similar location of three individual animals per experimental group, using

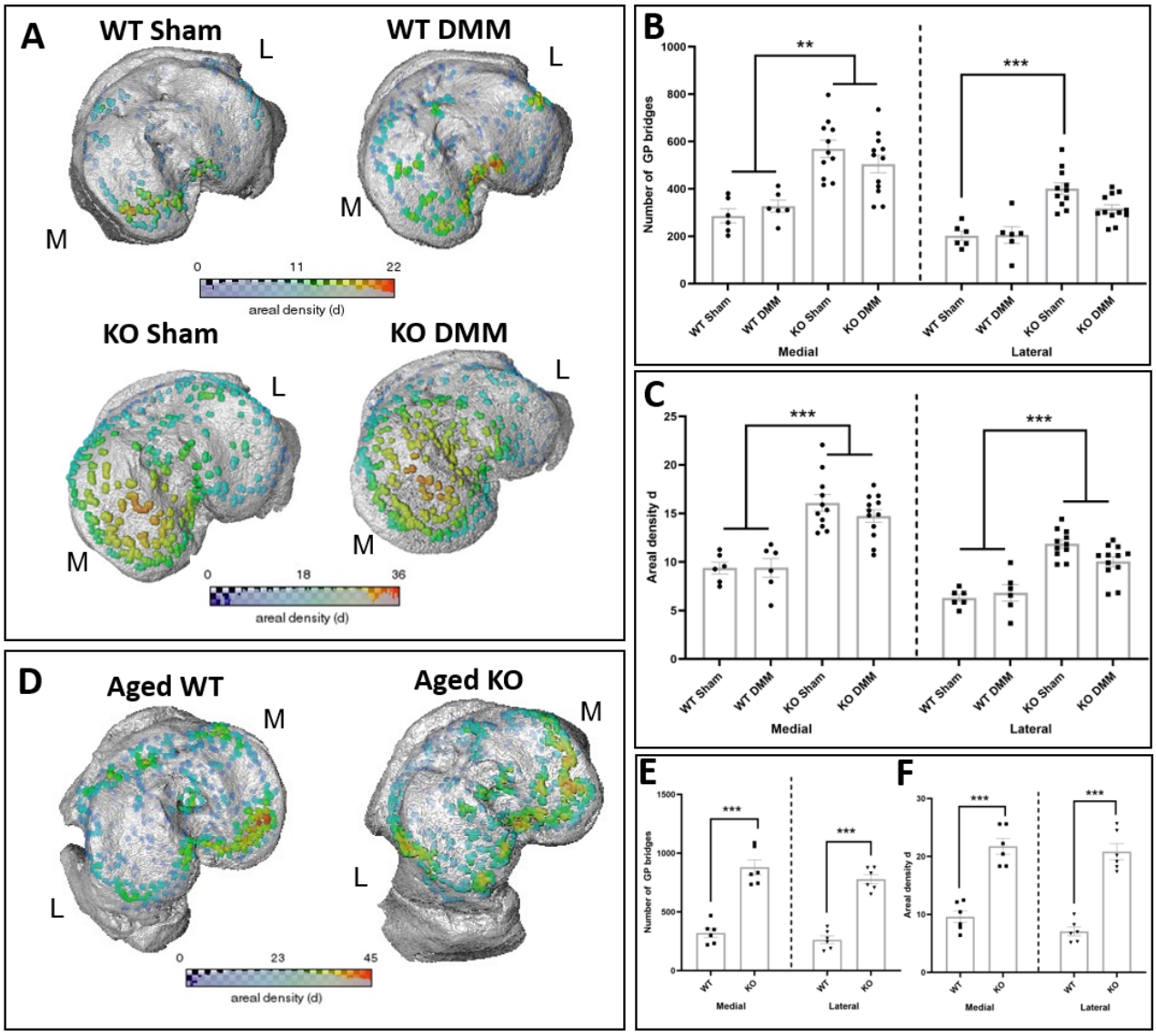

Fig. 2

Socs2-deficient mice exhibit accelerated growth plate fusion mechanisms. a) Location and areal densities of bridges across the growth plate projected on the medial (M) and lateral (L) tibial joint surface in wild type (WT) and Socs2$^{-/-}$ (knockout (KO)) destabilization of medial meniscus (DMM) and sham-operated joints. b) Number of growth plate (GP) bridges. c) Areal density of bridges defined as the number of bridges per 256 mm × 256 mm window. d) Location and areal densities of bridges across the growth plate projected on the medial (M) and lateral (L) tibial joint surface in aged WT and Socs2$^{-/-}$ (KO) mice. e) Number of GP bridges. f) Areal density (d) of bridges, defined as the number of bridges per 256 mm × 256 mm window. Data are presented as mean and standard error of the mean, and showing individual animals. Two-way analysis of variance with Bonferroni adjustments for multiple comparisons was used within each joint compartment. *p < 0.05; **p < 0.01; ***p < 0.001.

a light microscope and ImageJ (National Institutes of Health, USA) software. Articular cartilage damage was assessed in the medial tibia using the well-established Osteoarthritis Research Society International (OARSI) grading scale, with scores averaged.[20] Osteophytes were also scored where 0 = none; 1 = formation of cartilage-like tissue; 2 = increase in cartilaginous matrix; 3 = endochondral ossification.[21] Scoring was conducted blindly by two observers (HJS and KAS).

Statistical analysis. All analyses were performed with GraphPad Prism software 6.0 f version (GraphPad, USA). The results were presented as the mean and standard error of the mean (SEM). Normal distribution of data was assessed using the Shapiro-Wilk normality test. For the growth plate bridging and micro-CT analysis, one- or two-way analysis of variance (ANOVA) with Bonferroni adjustments for multiple comparisons were used, and independent-samples *t*-test was used for ageing studies. For articular cartilage damage, the Kruskal-Wallis one-way ANOVA was used for DMM studies, and the Mann-Whitney U test for ageing studies. The significance was set at $p < 0.05$.

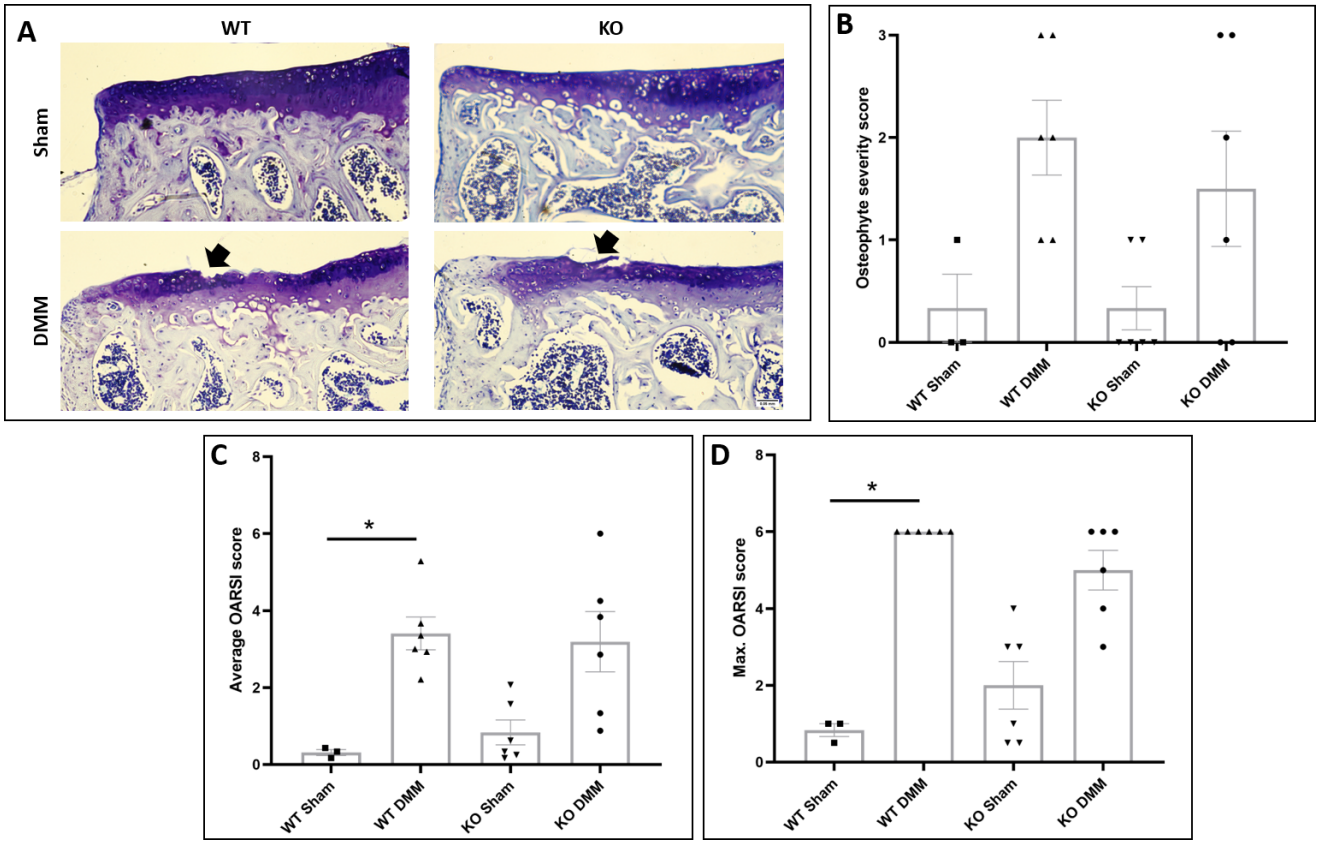

Fig. 3

Deletion of Socs2 does not prevent osteoarthritic articular cartilage lesions in a surgical model of osteoarthritis. a) Toluidine blue stained sections of the knee joint of wild type (WT) and Socs2$^{-/-}$ (knockout (KO)) mice showing development of articular cartilage lesions in the medial tibia (10×). b) Osteophyte severity score, c) mean articular cartilage damage Osteoarthritis Research Society International (OARSI) score,[20] and d) maximum articular cartilage damage OARSI score in WT sham (n = 3), WT destabilization of the medial meniscus (DMM) (n = 6), KO sham (n = 6), and KO DMM (n = 6). Scale bar = 0.05 mm. Data are presented as mean and standard error of the mean, showing individual animals; Kruskal-Wallis one-way analysis of variance was used.

Results

Socs2$^{-/-}$ mice exhibit accelerated growth plate fusion. In accordance with the known effects of increased GH signalling on the skeleton, we observed a significant increase in *Socs2*$^{-/-}$ body weight in comparison to WT controls in ageing (Socs2$^{-/-}$ 51.9 g (SD 1.4); WT 32.0 g (SD 0.5); p = 0.000; independent-samples *t*-test), and throughout the eight-week DMM experiment (Table I; p < 0.001; independent-samples repeated measures *t*-test). We also observed widened growth plates in our *Socs2*$^{-/-}$ mice, in comparison to WT in the DMM experiment, specifically in the proliferative zone of chondrocytes, as in accordance with previous studies at a younger age (Figures 1a and 1b).[19] However, no differences were observed in aged animals (Figures 1b and 1f).

We next sought to examine growth plate fusion in these mice. We observed a significant increase in the number of growth plate bridges in *Socs2*$^{-/-}$ mice in comparison to WT mice at both ages examined (Figure 2 and Supplementary Figure a). Specifically, we saw a significant increase in growth plate bridge number (Figure 2) (WT DMM: 532 (SD 56); WT sham: 495 (SD 45); knockout (KO) DMM: 169 (SD 49); KO sham: 187 (SD 56); p < 0.001, two-way ANOVA) and density (Figures 2a and 2c) (WT DMM: 2.2 (SD 0.9); WT sham: 1.2 (SD 0.5); KO DMM: 13.0 (SD 0.5); KO sham: 14.4 (SD 0.7); p < 0.001, two-way ANOVA) in *Socs2*$^{-/-}$ sham and DMM tibiae (16 weeks of age), in comparison to WT sham and DMM tibiae . Further, we saw no significant differences between growth plate bridges in the medial and lateral condyles in WT animals, however in *Socs2*$^{-/-}$ there is a significant reduction in growth plate bridge number and density in the lateral condyle, regardless of OA development (p < 0.001, two-way ANOVA (Figures 2b and 2c)). No differences in growth plate bridges were observed with OA development in either genotype. Concurrent with this, in aged mice (around one year), a significant increase in growth plate bridge number (Figures 2d and 2e) and density (Figures 2d and 2f) was observed in *Socs2*$^{-/-}$ mice in comparison to WT mice (WT: 585 (SD 70); KO: 1,659 (SD 91); densities – WT: 8.6 (SD 2.2); KO: 21.3 (SD 1.4); p < 0.001, two-way ANOVA).

Socs2 deletion does not exacerbate the development of OA in a DMM model. Assessment of cartilage damage in the medial tibia of WT mice revealed an increased articular cartilage OARSI score with DMM in comparison to

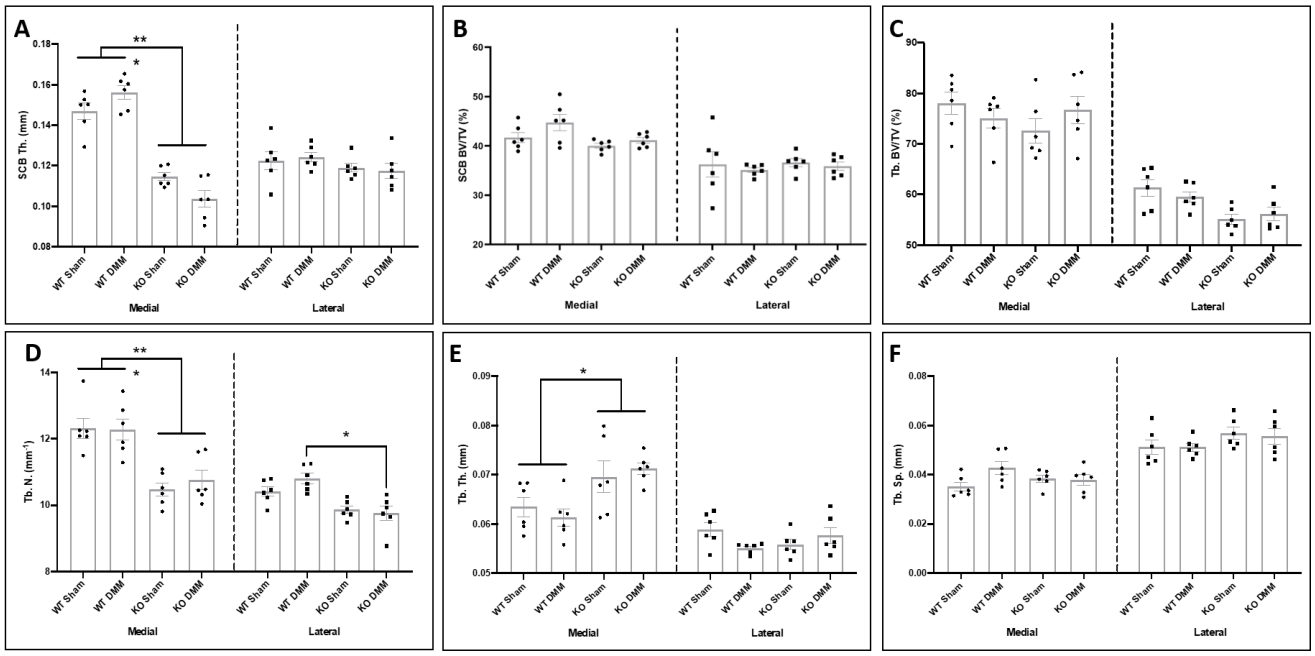

Fig. 4

Socs2-deficient mice exhibit decreased subchondral bone plate and trabecular number, irrespective of destabilization of the medial meniscus (DMM) surgically induced osteoarthritis. Micro-CT analysis of the medial and lateral tibial a) subchondral bone plate (SCB) thickness (mm), b) SCB bone volume/tissue volume (BV/TV; %), c) epiphyseal trabecular BV/TV (%), d) epiphyseal trabecular number (mm^{-1}), e) epiphyseal trabecular thickness (mm), and f) epiphyseal trabecular separation (mm) in wild type (WT) and $Socs2^{-/-}$ (knockout (KO)) mice with DMM or sham surgery (n = 6 per group). Data are presented as mean and standard error of the mean and show individual animal data. Two-way analysis of variance with Bonferroni adjustments was used for multiple comparisons. *p < 0.05; ***p < 0.001.

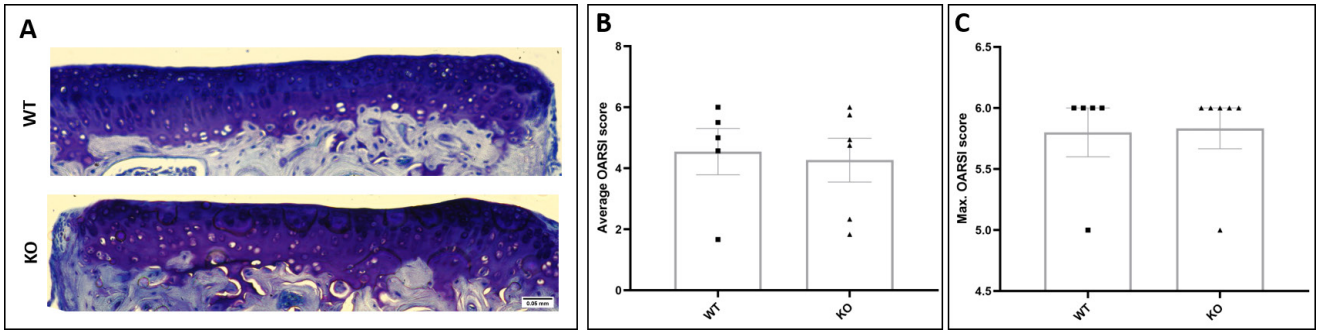

Fig. 5

Deletion of Socs2 does not prevent osteoarthritic articular cartilage lesions from ageing. a) Toluidine blue stained sections of the knee joint of 12- to 13-month-old WT and $Socs2^{-/-}$ (knockout (KO)) mice showing development of articular cartilage lesions in the medial tibia (10×). b) Mean articular cartilage damage Osteoarthritis Research Society International (OARSI) score across the knee joint and c) maximum articular cartilage damage OARSI score between wild type (WT) (n = 5) and KO (n = 6) mice with ageing, in the medial tibia of the knee joint. Scale bar = 0.05 mm. Data are presented as mean and standard error of the mean, and show individual animals; Mann-Whitney U test was used.

sham (p < 0.050, Kruskal-Wallis one-way ANOVA; Figures 3a, 3c, and 3d). However, no significant differences in the articular cartilage mean and maximum OARSI severity scores were observed between WT and *Socs2*$^{-/-}$ mice in the medial tibia (no significant difference (Figures 3c and 3d)). Similar results were observed in the lateral tibia (data not shown). Similarly, while osteophytes were observed in both WT and *Socs2*$^{-/-}$ DMM mice, there was no difference between genotypes (Figure 3b). Micro-CT analysis of the subchondral bone plate revealed a significantly thinner subchondral bone plate in the medial compartment of *Socs2*$^{-/-}$ knee joints, in comparison to WT knee joints (Figure 4a; SCB Th. WT: 0.15 mm (SD 0.003); KO: 0.11 mm (SD 0.003); p < 0.001, two-way ANOVA). DMM had no effect on the subchondral bone plate thickness in comparison to sham in either WT or $Socs2^{-/-}$ knee joints (Figure 4a). Similarly, no differences were observed in the subchondral bone % BV/TV between genotypes or OA interventions (Figure 4b). Micro-CT analysis of the epiphyseal trabecular bone also revealed no effect of DMM on % BV/TV (Figure 3c), however we observed decrease in trabecular number (Figure 4d; Tb. N. WT: 12.3 mm^{-1}

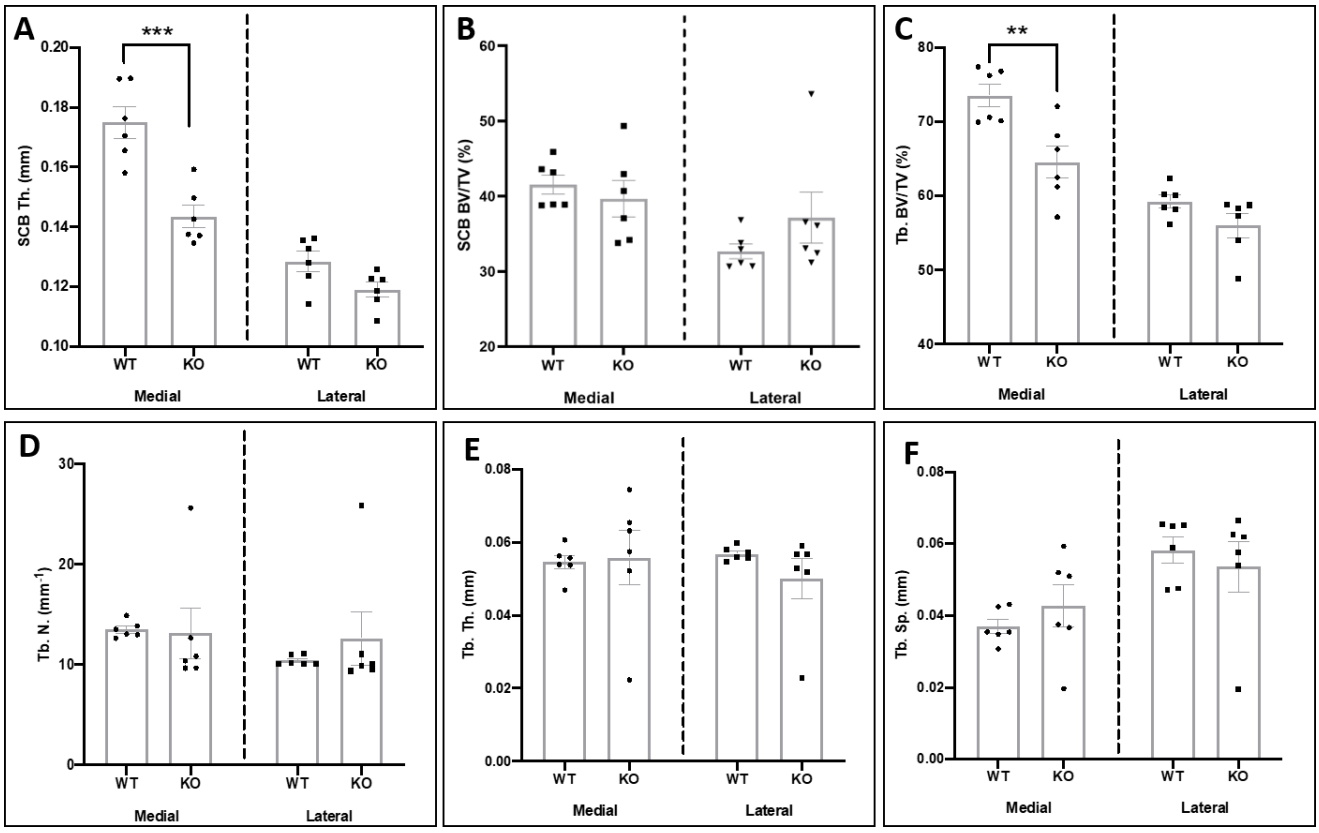

Fig. 6

Aged Socs2-deficient mice exhibit decreased subchondral bone plate thickness. Micro-CT analysis of the medial and lateral tibial a) subchondral bone plate (SCB) thickness (mm), b) SCB bone volume/tissue volume (BV/TV; %), c) epiphyseal trabecular BV/TV (%), d) epiphyseal trabecular number (mm^{-1}), e) epiphyseal trabecular thickness (mm), and f) epiphyseal trabecular separation (mm) in aged wild type (WT) and $Socs2^{-/-}$ (knockout (KO)) mice (n = 6 per group). Data are presented as mean and standard error of the mean, and show individual animals. Two-way analysis of variance with Bonferroni adjustments for multiple comparisons was used. *p < 0.05; ***p < 0.001.

(SD 0.2); KO: 10.6 mm^{-1} (SD 0.2); p < 0.001, two-way ANOVA) and increase in trabecular thickness (Figure 4e; Tb. Th. WT: 0.06 mm (SD 0.001); KO: 0.07 mm (SD 0.002); p = 0.007, two-way ANOVA) in *Socs2*$^{-/-}$ knee joints in comparison to WT knee joints. DMM had no effect on the epiphyseal bone parameters in comparison to sham, in either WT or *Socs2*$^{-/-}$ knee joints (Figures 4c to 4f).

Socs2 deletion has no effect on joint ageing. To examine the effects of *Socs2* deletion in aged joints, histological examination revealed no differences in the articular cartilage lesion mean and maximum severity scores between aged WT and $Socs2^{-/-}$ mice in any of the joint compartments (Figures 5a to 5c). Similar to our previous analysis of DMM-treated WT and *Socs2*$^{-/-}$ mice (Figure 4), micro-CT analysis of the subchondral bone revealed thinner subchondral bone plate in the medial compartment of *Socs2*$^{-/-}$ knee joints, in comparison to WT knee joints (Figure 6a; SCB Th. WT: 0.2 mm (SD 0.005); KO: 0.1 mm (SD 0.004); p < 0.001, two-way ANOVA). No differences were observed in the subchondral bone % BV/TV between genotypes (Figure 6b), however the epiphyseal trabecular BV/TV was decreased in *Socs2*$^{-/-}$ knee joints (Figure 6c; Tb. BV/TV WT: 73.5% (SD 1.5%); KO: 64.6% (SD 2.2%); p = 0.001, two-way ANOVA). No significant differences were observed in trabecular number (Figure 6d), trabecular thickness (Figure 6e), or trabecular separation (Figure 6f) between aged WT and $Socs2^{-/-}$ mice.

Discussion

Here we sought to examine whether altered growth plate dynamics underpin OA through examination of OA vulnerability in a murine model of accelerated growth (*Socs2*$^{-/-}$). We describe accelerated growth plate fusion in these mice, consistent with their known overgrowth phenotype. However, we found no effect of surgical intervention or ageing on the articular cartilage or subchondral bone phenotype in these mice. This suggests that in this murine model, aberrant growth dynamics are not associated with vulnerability to OA development.

It is well established that in OA, chondrocytes in the articular cartilage adopt a more transient phenotype, similar to that seen in the growth plate.[22] This raises the question as to whether a greater understanding of the discordant chondrocyte phenotype may inform on mechanisms underpinning OA, and strategies for treatment. Staines et al[11] have shown that in a spontaneous model of OA (STR/Ort mouse), there is an association between aberrant growth plate dynamics and OA development.

Specifically, they revealed that STR/Ort mice show an overgrowth phenotype with enriched growth plate bridging, which was associated with articular cartilage lesions at 18 to 20 weeks of age.[11] This is similar to the growth phenotype observed in the *Socs2*$^{-/-}$ described herein. Further, previous work on the MRC National Survey of Health and Development revealed modest associations between greater gains in height in childhood and decreased risk of knee OA at 53 years.[23] Further, canine studies have shown that femoral lengthening by 30% leads to knee articular cartilage damage, which is protected by apparatus extension with a hinged fixation system to the tibia.[24] Together, this suggests that an accelerated growth rate may play a role in the development of OA, although what that role is has yet to be fully defined.

SOCS2 is a negative regulator of GH signalling, via inhibition of the Janus kinase/signal transducers and activators of transcription (JAK/STAT) pathway.[25] Thus, mice deficient in *Socs2*$^{-/-}$ display an excessive growth phenotype.[16] Characterization of their growth phenotype has revealed increased bone growth rates, growth plate widths, and chondrocyte proliferation in *Socs2*$^{-/-}$ six-week-old mice compared to age-matched WT mice, suggestive of accelerated growth.[26] *Socs2*$^{-/-}$ mice have normal serum levels of GH and insulin-like growth factor-1 (IGF-1), and their longitudinal overgrowth phenotype is due to local effects of the GH/IGF-1 axis on the growth plate.[27] Consistent with this, we revealed increased numbers and densities of growth plate bridges in *Socs2*$^{-/-}$ mice, in comparison to WT mice. Growth plate bridges form in coordination with chondrocytes of the growth plate, exhausting their proliferative potential and undergoing senescence. They are also known to form upon growth plate injury, thought to be through an intramembranous ossification mechanism.[28] However, whether growth plate fusion occurs prior to or after the cessation of growth is of significant controversy in the field and has been somewhat overlooked.[9]

Using finite element modelling, work by Madi et al[18] and Staines et al[8] has previously shown growth plate bridging to increase stress dissipation in the subchondral bone region of the joint. It is therefore surprising that the increased growth plate bridging observed in our *Socs2*$^{-/-}$ mice here had reduced subchondral bone plate and trabecular parameters. Previous studies have examined the *Socs2*$^{-/-}$ bone phenotype with contradictory results. Our previous work has shown that *Socs2*$^{-/-}$ mice have increased bone mass, trabecular number, and trabecular thickness.[17,27] However, others have shown the absence of SOCS2 to induce losses in cortical and trabecular bone mineral density.[29] These results are not consistent with the expected augmented GH/IGF-1 axis, but are consistent with our findings here and highlight the complexity of this pathway and the need for further studies to elucidate the precise role of SOCS2 signalling in bone homeostasis.

Increased GH but reduced IGF-1 concentrations are present in synovial fluid of patients with OA.[30] However, in rodents deficient in GH and IGF-1, an increased severity of osteoarthritic articular cartilage lesions is observed.[31] Further, it has previously been shown that *Socs2* messenger RNA (mRNA) levels are decreased in chondrocytes from osteoarthritic femoral heads.[32] Together, these data suggest a role for the GH/IGF-1/SOCS2 pathway in the pathology of OA. However, our results indicate that there is no effect of SOCS2 deficiency on OA vulnerability. This may be due to the normal serum levels of GH/IGF-1 observed in *Socs2*$^{-/-}$ mice,[27] and suggests that compensatory cellular mechanisms exist in the *Socs2*$^{-/-}$ which may involve other SOCS members. Indeed, eight SOCS proteins have been identified, and work by de Andrés et al[32] suggests that SOCS1 and SOCS3 are likely to play such a compensatory role. Further, the GH/IGF-1 status of the STR/Ort mouse, which exhibits a similar overgrowth phenotype to the *Socs2*$^{-/-}$ mice but with spontaneous OA development, is unknown, and this may provide further insights into this mechanism. Similarly, we know that the GH signalling pathway is extremely complex, thus highlighting the need to better understand GH/IGF-1 signalling in the aetiology of OA.

In summary, our data show that deletion of SOCS2 leads to accelerated growth plate fusion, but this had no effect on OA vulnerability in a surgical model of murine OA. Future studies will determine whether this lack of vulnerability is specific to this model of accelerated longitudinal growth, or whether this is characteristic of OA in general.

Twitter

Follow H. J. Samvelyan @JSamvelyan
Follow C. Huesa @CHuesa
Follow K. A. Staines @Dr_KatherineS

Supplementary material

Figure displaying identification of bony bridges crossing the epiphyseal growth plate. An ARRIVE checklist is also included to show that the ARRIVE guidelines were adhered to in this study.

References

1. **Glasson SS**, **Askew R**, **Sheppard B**, **et al**. Deletion of active ADAMTS5 prevents cartilage degradation in a murine model of osteoarthritis. *Nature*. 2005;434(7033):644–648.
2. **Echtermeyer F**, **Bertrand J**, **Dreier R**, **et al**. Syndecan-4 regulates ADAMTS-5 activation and cartilage breakdown in osteoarthritis. *Nat Med*. 2009;15(9):1072–1076.
3. **Saito T**, **Fukai A**, **Mabuchi A**, **et al**. Transcriptional regulation of endochondral ossification by HIF-2alpha during skeletal growth and osteoarthritis development. *Nat Med*. 2010;16(6):678–686.
4. **Wang M**, **Sampson ER**, **Jin H**, **et al**. MMP13 is a critical target gene during the progression of osteoarthritis. *Arthritis Res Ther*. 2013;15(1):R5.
5. **Chang SH**, **Mori D**, **Kobayashi H**, **et al**. Excessive mechanical loading promotes osteoarthritis through the gremlin-1–NF-κB pathway. *Nat Commun*. 2019;10(1):1–5.
6. **Kronenberg HM**. Developmental regulation of the growth plate. *Nature*. 2003;423(6937):332–336.
7. **Nagao M**, **Hamilton JL**, **Kc R**, **et al**. Vascular endothelial growth factor in cartilage development and osteoarthritis. *Sci Rep*. 2017;7(1):1–16.
8. **Staines KA**, **Madi K**, **Javaheri B**, **Lee PD**, **Pitsillides AA**. A computed microtomography method for understanding epiphyseal growth plate fusion. *Front Mater*. 2018;4:48.

9. **Parfitt AM**. Misconceptions (1): epiphyseal fusion causes cessation of growth. *Bone*. 2002;30(2):337–339.
10. **Aigner T**, **Zhu Y**, **Chansky HH**, **Matsen FA**, **Maloney WJ**, **Sandell LJ**. Reexpression of type IIA procollagen by adult articular chondrocytes in osteoarthritic cartilage. *Arthritis Rheum*. 1999;42(7):1443–1450.
11. **Staines KA**, **Madi K**, **Mirczuk SM**, **et al**. Endochondral growth defect and deployment of transient chondrocyte behaviors underlie osteoarthritis onset in a natural murine model. *Arthritis Rheumatol*. 2016;68(4):880–891.
12. **Samvelyan HJ**, **Hughes D**, **Stevens C**, **Staines KA**. Models of osteoarthritis: relevance and new insights. *Calcif Tissue Int*. 2021;109(3):243–256.
13. **Letellier E**, **Haan S**. SOCS2: physiological and pathological functions. *Front Biosci (Elite Ed)*. 2016;8(1):189–204.
14. **Keating N**, **Nicholson SE**. SOCS-mediated immunomodulation of natural killer cells. *Cytokine*. 2019;118:64–70.
15. **Cramer A**, **de Lima Oliveira BC**, **Leite PG**, **et al**. Role of SOCS2 in the Regulation of Immune Response and Development of the Experimental Autoimmune Encephalomyelitis. *Mediators Inflamm*. 2019;2019:1872593.
16. **Metcalf D**, **Greenhalgh CJ**, **Viney E**, **et al**. Gigantism in mice lacking suppressor of cytokine signalling-2. *Nature*. 2000;405(6790):1069–1073.
17. **Dobie R**, **MacRae VE**, **Pass C**, **Milne EM**, **Ahmed SF**, **Farquharson C**. Suppressor of cytokine signaling 2 (*Socs2*) deletion protects bone health of mice with DSS-induced inflammatory bowel disease. *Dis Model Mech*. 2018;11(1):dmm028456.
18. **Madi K**, **Staines KA**, **Bay BK**, **et al**. In situ characterization of nanoscale strains in loaded whole joints via synchrotron X-ray tomography. *Nat Biomed Eng*. 2020;4(3):343–354.
19. **Hunziker EB**, **Schenk RK**, **Cruz-Orive LM**. Quantitation of chondrocyte performance in growth-plate cartilage during longitudinal bone growth. *J Bone Joint Surg Am*. 1987;69-A(2):162–173.
20. **Glasson SS**, **Chambers MG**, **Van Den Berg WB**, **Little CB**. The OARSI histopathology initiative - recommendations for histological assessments of osteoarthritis in the mouse. *Osteoarthritis Cartilage*. 2010;18 Suppl 3:S17-23.
21. **Nagira K**, **Ikuta Y**, **Shinohara M**, **et al**. Histological scoring system for subchondral bone changes in murine models of joint aging and osteoarthritis. *Sci Rep*. 2020;10(1):10077.
22. **Pitsillides AA**, **Beier F**. Cartilage biology in osteoarthritis--lessons from developmental biology. *Nat Rev Rheumatol*. 2011;7(11):654–663.
23. **Staines KA**, **Hardy RJ**, **Samvelyan HJ**, **Ward KA**, **Cooper R**. Life course longitudinal growth and risk of knee osteoarthritis at age 53 years: evidence from the 1946 British birth cohort study. *Osteoarthritis Cartilage*. 2021;29(3):335–340.
24. **Stanitski DF**, **Rossman K**, **Torosian M**. The effect of femoral lengthening on knee articular cartilage: the role of apparatus extension across the joint. *J Pediatr Orthop*. 1996;16(2):151–154.
25. **Pass C**, **MacRae VE**, **Ahmed SF**, **Farquharson C**. Inflammatory cytokines and the GH/IGF-I axis: novel actions on bone growth. *Cell Biochem Funct*. 2009;27(3):119–127.
26. **Pass C**, **MacRae VE**, **Huesa C**, **Faisal Ahmed S**, **Farquharson C**. SOCS2 is the critical regulator of GH action in murine growth plate chondrogenesis. *J Bone Miner Res*. 2012;27(5):1055–1066.
27. **Macrae VE**, **Horvat S**, **Pells SC**, **et al**. Increased bone mass, altered trabecular architecture and modified growth plate organization in the growing skeleton of SOCS2 deficient mice. *J Cell Physiol*. 2009;218(2):276–284.
28. **Xian CJ**, **Zhou FH**, **McCarty RC**, **Foster BK**. Intramembranous ossification mechanism for bone bridge formation at the growth plate cartilage injury site. *J Orthop Res*. 2004;22(2):417–426.
29. **Lorentzon M**, **Greenhalgh CJ**, **Mohan S**, **Alexander WS**, **Ohlsson C**. Reduced bone mineral density in SOCS-2-deficient mice. *Pediatr Res*. 2005;57(2):223–226.
30. **Denko CW**, **Boja B**, **Moskowitz RW**. Growth factors, insulin-like growth factor-1 and growth hormone, in synovial fluid and serum of patients with rheumatic disorders. *Osteoarthritis Cartilage*. 1996;4(4):245–249.
31. **Ekenstedt KJ**, **Sonntag WE**, **Loeser RF**, **Lindgren BR**, **Carlson CS**. Effects of chronic growth hormone and insulin-like growth factor 1 deficiency on osteoarthritis severity in rat knee joints. *Arthritis Rheum*. 2006;54(12):3850–3858.
32. **de Andrés MC**, **Imagawa K**, **Hashimoto K**, **et al**. Suppressors of cytokine signalling (SOCS) are reduced in osteoarthritis. *Biochem Biophys Res Commun*. 2011;407(1):54–59.

Author information:

- H. J. Samvelyan, MS, MRes, PhD, Lecturer, School of Pharmacy and Biomolecular Sciences, University of Brighton, Brighton, UK; Centre for Stress and Age-Related Disease, University of Brighton, Brighton, UK; The Faculty of Health, Education, Medicine and Social Care, School of Medicine, Anglia Ruskin University, Chelmsford, UK.
- C. Huesa, BSc, PhD, Research Fellow, Institute of Infection, Immunity & Inflammation, College of Medical, Veterinary and Life Sciences, University of Glasgow, Glasgow, UK.
- L. Cui, PhD, Postdoctoral Research Associate
- C. Farquharson, PhD, Professor of Skeletal Biology
  The Roslin Institute, The University of Edinburgh, Edinburgh, UK.
- K. A. Staines, BSc, PhD, Senior Lecturer, School of Pharmacy and Biomolecular Sciences, University of Brighton, Brighton, UK; Centre for Stress and Age-Related Disease, University of Brighton, Brighton, UK.

Author contributions:

- H. J. Samvelyan: Conceptualization, Investigation, Writing – original draft, Writing – review & editing.
- C. Huesa: Investigation, Writing – review & editing.
- L. Cui: Investigation, Writing – review & editing.
- C. Farquharson: Conceptualization, Writing – review & editing.
- K. A. Staines: Conceptualization, Investigation, Writing – original draft, Writing – review & editing.

Funding statement:

- This work was supported by the Medical Research Council (MR/R022240/2) and a University of Brighton Rising Star Award, both to K. A. Staines. C. Farquharson was supported by the Biotechnology and Biological Sciences Research Council (BBSRC) via an Institute Strategic Programme Grant (BB/J004316/1). C. Huesa is supported by an early career fellowship from Versus Arthritis (22483).

Data sharing:

- Data are available upon reasonable request to the corresponding author.

Acknowledgements:

- The authors would like to thank Dr Blandine Poulet of University of Liverpool, Institute of Ageing and Chronic Disease, for her guidance in experimental techniques and insightful discussions throughout preparation. We also thank Dr Kamel Madi for his assistance with the generation of Supplementary Figure a.

Ethical review statement:

- All experimental protocols were approved by the local ethics committee, and the animals were maintained in accordance with UK Home Office guidelines for the care and use of laboratory animals. Animal studies were conducted in line with the ARRIVE guidelines.

Open access funding

- Open access funding for this study was provided by the University of Brighton UKRI Open Access Publication Fund.